COMPLEX RESISTIVITY OF FAULT GOUGE AND ITS SIGNIFICANCE FOR EARTHQUAKE LIGHTS AND INDUCED POLARIZATION

David A. Lockner and James D. Byerlee

U.S. Geological Survey, Menlo Park, CA

Abstract. We have measured complex resistivity of 2 water-saturated San Andreas fault gouges from 10^{-3} to 10^{6} Hz and confining pressures of 0.2 to 200 MPa. Consistent with earlier observations of clays and common rocks, large low-frequency permittivities were observed in all cases. Comparisons were made to induced polarization (IP) measurements by inversion of the data into the time domain, where we found that principal features of the IP response curves were due to these large low-frequency permittivities. The results also suggest that following large earthquakes, significant electrical charge could remain for many seconds and could result in a variety of reported electromagnetic effects.

Introduction

The existance of earthquake lights (EQL) has long been debated in the scientific community, despite an accumulation of numerous, albeit untrained, eye-witness accounts [Derr, 1973]. A number of mechanisms have been proposed by which an earthquake could generate sizable electrical charge. These include frictional heating of the fault [Lockner et al., 1983], piezoelectric effects [Finkelstein and Powell, 1970], and streaming potential [Mitzutani et al., 1976]. While the generation and concentration of electrical charge by an earthquake can be adequately supported both theoretically and experimentally [Lockner et al., 1983], the major objection to EQL has been that any generated charge would dissipate far too quickly in a conductive Earth to allow time for the reported phenomena to occur. This argument has been presented in the following manner. The electric field E created by the generation of an electrostatic charge, will decrease [Madden and Williams, 1976] at a rate

$$E = E_o \exp(-\sigma t/\varepsilon_o K) \qquad (1)$$

where σ is conductivity, ε_o is permittivity of free space and K is relative permittivity of the material. σ of common wet rocks is about 10^{-2} S m^{-1} and K, generally measured at high frequency and/or for dry samples, is about 10. The resulting microsecond relaxation time is too short to allow for the accumulation of significant charge. A solution to this problem was given by Lockner et al. [1983] in which frictional heating of the fault was sufficient to vaporize pore water and thereby reduce σ by many orders of magnitude. In this paper, we will extend our earlier results by showing that for wet rocks, K is in general frequency dependent. We will present the results of direct measurements of the frequency dependence of σ and K for samples of San Andreas fault gouge as well as some common rock types. When these measurements are inverted into the time domain, the very large low-frequency permittivities result in transient decays that last for many seconds. This time domain response bears close resemblance to conventional induced polarization (IP) response curves. In fact, we suggest a close relationship between IP response mechanisms and the decay of charge accompanying some earthquakes.

Paper number 4L6420.

Sample Descriptions

Two samples of San Andreas fault gouge were tested. One was a clay-rich gouge we will refer to as DLV, taken from the Dry Lake Valley drill hole at a depth of 186 to 189 m, and has an approximate percent composition of montmorillonite and mixed-layer clays: 43, kaolinite: 39, illite: 10 and chlorite: 8. A second gouge sample BP, taken from an exposure of the fault zone near Big Pines in the San Gabriel mountains, is derived from granite gneiss and has virtually no clay content, although it contains a high percentage of clay-sized particles. This sample is referred to as BP5 in Anderson et al. [1980]. Two other samples, Westerly granite (WES) and Berea sandstone (BER), were also measured. The results of these latter 2 experiments will be presented in detail in a later report.

Experimental Procedure

A solution of 0.01 molar KCl in distilled, deionized water (7.1 ohm-m) was used to saturate all samples. Gouges were initially mixed, by weight, with 29% (DLV) and 21% (BP) electrolyte. Resistivity of the fluid expelled by sample DLV as it compacted was 0.8 ohm-m, indicating that high-solubility salts were leached out of this sample. Gouge samples were packed in 2.54 cm diameter vinyl jackets and sandwiched between Pt electrodes (coated with Pt-black) and porous Al_2O_3 spacers. Initial sample lengths for DLV and BP were 1.17 and 1.37 cm, respectively. 2.54 cm diameter cylindrical cores of granite and sandstone were jacketed in a similar manner. A 4-electrode technique was employed to measure complex resistivity over the range in frequency from 10^{-3} to 10^{2} Hz [Olhoeft, 1979]. At higher frequencies (10^{2} to 10^{6} Hz) where electrode polarization was not significant, a two-electrode technique, using Hewlett Packard LCR meters, was used. These instruments are designed to measure sample impedance at prescribed frequencies and excitation potentials.

TABLE 1. Sample Parameters at 1 Hz

	P_{conf} MPa	Poros. %	ρ' ohm-m	φ mrad	σ' S m^{-1}	K' X10^6
DLV	1	42	4.945	- 3.5	0.2022	13
	12	31	7.493	- 4.3	0.1335	10
	100	23	15.52	- 6.3	0.06444	7.3
	200	18	28.54	- 8.5	0.03504	5.4
BP	1	24	9.25	-10.3	0.1082	20
	20	16	10.85	-10.6	0.09215	18
	100	8	20.91	-11.2	0.04783	9.6
	174	5	41.69	- 7.1	0.02398	3.1
WES	100	~.08	47691.	-23.2	$2.096X10^{-5}$	0.0087
BER	100	18	122.3	-8.7	0.008177	1.3

Samples were placed in a pressure vessel and measurements taken from 0.2 to 200 MPa confining pressure. Pore pressure was vented to the atmosphere. Samples were allowed to equilibrate from 3 to 50 hrs between measurements. Compaction of gouge samples was calculated by measurement of fluid expelled and, above 10 MPa, by measurement of axial shortening of the sample. Due to uncertainties in sample dimensions caused by barreling, absolute resistivities of the gouge samples are known to approximately 10% accuracy, although relative frequency response at a given pressure is accurate in general to 0.2%.

Results

We will use the following quantities to present our data: complex resistivity $\rho^*=\rho'-i\rho''$ where $i=(-1)^{1/2}$; complex conductivity $\sigma^*=\sigma'+i\sigma''$ and complex relative permittivity $K^*=K'-iK''$ which are related by

$$\sigma^* = i\omega\varepsilon_o K^* = (\rho^*)^{-1} \quad . \qquad (2)$$

$\omega=2\pi f$ is angular frequency. Then dissipation factor D or loss tangent tan δ are related by

$$D = \tan\delta = \sigma'/\sigma'' = \rho'/\rho'' = K''/K' \quad . \qquad (3)$$

We also define the phase angle $-\phi$ by which current leads voltage, so that $\phi=\delta-\pi/2$. We have made no distinction here as to the mechanisms that result in the observed frequency response. Whether we are dealing with high frequency electron orbital polarization or with low frequency electrochemical polarization, phenomenologically, polarization mechanisms behave similarly and, for our purposes are lumped together. Thus, the measurable quantities sometimes referred to as effective conductivity and effective permittivity are, in this paper, σ' and K'.

Values of some of the key parameters measured at 1 Hz are listed in Table 1. Since the general form of the response functions show only minor variations with confining pressure, we will present the complete response functions at a representative pressure of 100 MPa. Log ρ' and $-\phi$ of the 4 samples are plotted vs. log f in Figure 1. ρ' curves are offset vertically for clarity; see Table 1 for absolute values. Only minor variations in ρ' are observed at low frequency while the samples exhibit more variation in their phase response. All of the samples have low-frequency phase angles in the range 5 to 15 milliradians, representing an out-of-phase current of 0.5 to 1.5%. This requires a very large effective permittivity. Thus, when recomputed in terms of log σ' (Figure 2a) and log K' (Figure 2b), we find that while σ' shows some frequency dependence over this range of measurements, the strong low-frequency dispersion of K' is the dominant feature in all of the samples. This phenomenon has been reported for many wet geological materials [Howell and Licastro, 1961; Arulanandan and Mitchell, 1968; Shahidi et al., 1975; Lockhart, 1980; Keller, 1982] and is due to a variety of interfacial interactions that result in polarization of grain boundaries. A result of this frequency dependence is that, in contrast to the example for constant σ' and K' used in eq. (1), the time decay of E is not exponential. For materials with frequency dependent σ' and K', the decay function can be calculated in the following way. For a linear system, as is the case for all of these samples at the low current densities used, current density $\underline{J}(\omega)$ is related to electric field $\underline{E}(\omega)$ by the system transfer function (complex resistivity):

$$\underline{E}(\omega) = \rho^*(\omega)\ \underline{J}(\omega) \quad . \qquad (4)$$

For a given input current signal $\underline{j}(t)$, we take the discrete Fourier Transform DFT to obtain its

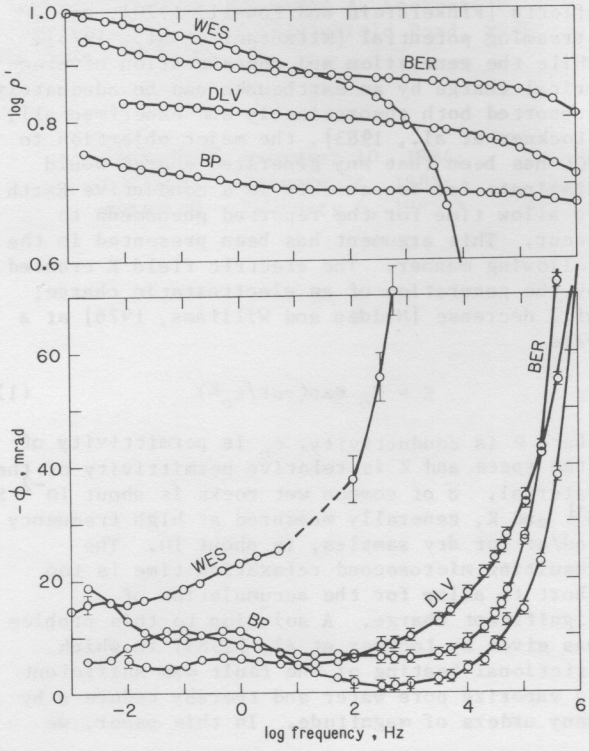

Fig. 1. a) Log ρ' and b) $-\phi$ of the 4 samples at 100 MPa confining pressure. Resistivities are offset vertically for clarity; see Table 1 for absolute values.

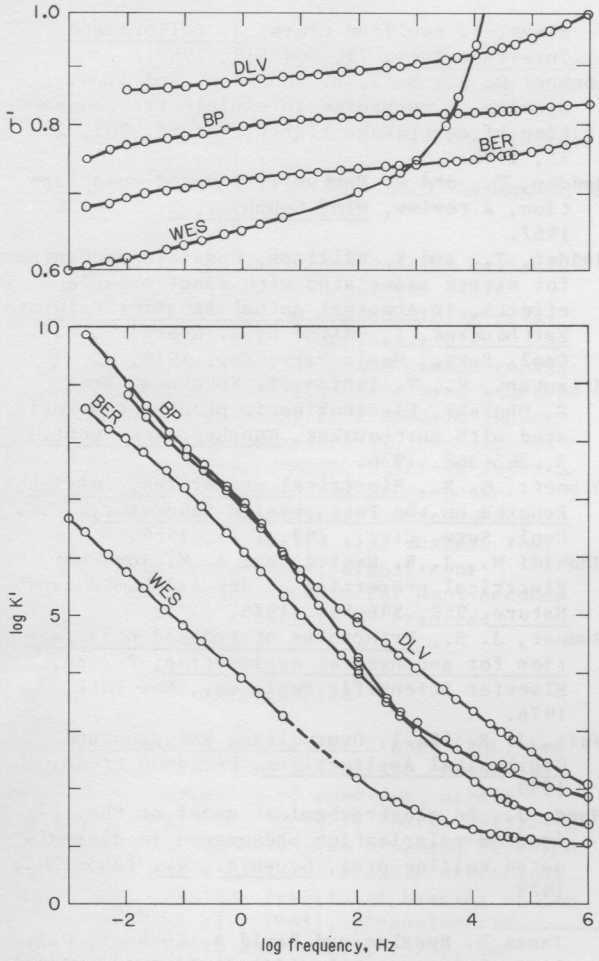

Fig. 2. a) Log σ' and b) log K' of the 4 samples at 100 MPa computed from values in Figure 1. σ' curves are offset vertically for clarity.

frequency content $\underline{J}(\omega)$, multiply by $\rho^*(\omega)$ and then take the inverse transform to obtain the electric field time response $\underline{e}(t)$:

$$\underline{e}(t) = DFT^{-1} \{\rho^*(\omega)\ DFT(\underline{j}(t))\} . \qquad (5)$$

Similar approaches, using Fourier or Laplace transforms or combinations of exponential functions, have been discussed by Wait [1959], Madden and Cantwell [1967] and Wong [1979].

As an example, we use a square wave input current function of 100 s duration where

$$\underline{j}(t) = \begin{cases} 0, & 0 < t < 37.5 \text{ s} \\ -1, & 37.5 < t < 50 \\ 0, & 50 < t < 87.5 \\ 1, & 87.5 < t < 100 \end{cases} . \qquad (6)$$

The input function is divided into 2^{18} equal time steps to obtain 5 orders of magnitude of dynamic range. Results are plotted in Figure 3 in the form mV/V vs. log t as is often done with IP measurements collected during exploration for ore bodies. These relaxation curves in Figure 3 exhibit many of the characteristic features of IP response curves (two of which, taken from Wait, 1959, pp. 57 and 61 are plotted in the figure). The principal feature is a nearly linear decay over much of the record which is the result of a constant low-frequency phase angle ϕ, and consequently large low-frequency dispersion of permittivity. It is also interesting to note that even for the high conductivity DLV sample, measurable voltage remains 1 s after the current is shut off. IP response curves commonly show decay times of 1 s or more, even for so-called 'background' or 'normal' response. This requires measurable low-frequency phase angles and consequently large permittivities. Furthermore, the IP response time will, in general, significantly increase when the pulse duration time of the input signal is increased [Sumner, 1976]. Since this procedure essentially adds more low-frequency energy, it also indicates that large low-frequency permittivities are present.

The curves plotted in Figure 3 can also be used to infer the decay of a space charge generated during an earthquake. For the purposes of this discussion, we will ignore the complications introduced by the geometry of the source region, since this will not alter the general form of the decay curves. Let us consider an M=8 earthquake, which might typically have a stress drop of 5 MPa, a slip velocity of 50 cm s^{-1} and a total slip of 625 cm. If charge were generated at a constant rate over the 12.5 s of slip duration, the curves in Figure 3 would represent the decay of a point source of charge following the earthquake. While much of the charge quickly dissipates after the earthquake, as much as 0.5 to 1 percent can remain for many seconds. If the initial charge generated during the earthquake is large, then this residual charge may be large enough to cause significant electromagnetic effects. Also, if the source region has a relatively high resistivity, as in the case of wet but low porosity crystalline rocks (sample WES), the electrical potential that can be developed will be proportionately larger.

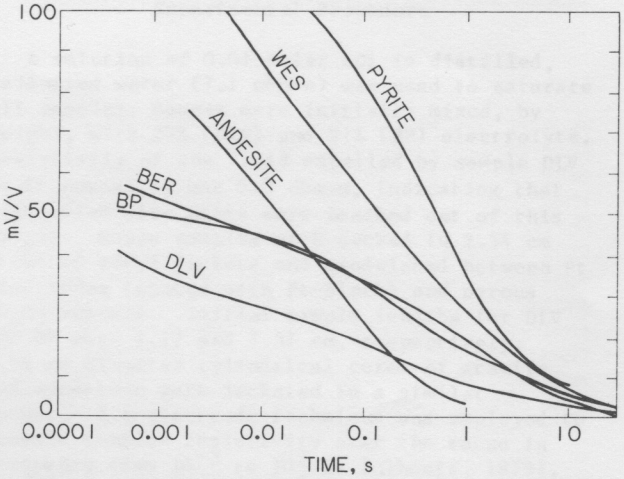

Fig. 3. Computed IP decay plots for the 4 samples in Figure 1 following a 12.5 s pulse (eq. 6). Also included are 2 IP decay curves [Pyrite and Andesite] measured directly in the laboratory [from Wait, 1959].

Conclusions

Frequency domain measurements of complex resistivity of fault gouges and country rocks at varying confining pressures have shown a large, low-frequency dispersion of permittivity in all cases. Inversion of this data into the time domain has enabled us to duplicate time domain IP measurements. One result of this exercise is to demonstrate that the principal feature of IP response curves, namely the long decay times, requires significant low-frequency phase angles, and consequently, large low-frequency dispersion of permittivity. This same phenomenon leads to the conclusion that for large earthquakes, significant residual localized charge can remain for many seconds, even in a wet, conductive Earth.

References

Anderson, J. L., R. H. Osborne, and D. F. Palmer, Petrogenesis of cataclastic rocks within the San Andreas fault zone of southern California, U.S.A., Tectonophys., 67, 221-249, 1980.

Arulanandan K., and J. Mitchell, Low frequency dielectric dispersion of clay-water-electrolyte systems, Clays and Clay Minerals, 16, 337-351, 1968.

Derr, J. S., Earthquake lights: a review of observations and present theories, Bull., Seism. Soc. Amer., 63, 2177-2187, 1973.

Finkelstein D., and J. Powell, Earthquake lightning, Nature, 228, 759-760, 1970.

Howell, B. F., and P. H. Licastro, Dielectric behavior of rocks and minerals, The Amer. Miner., 46, 269-288, 1961.

Keller, G. V., Electrical properties of rocks and minerals, in Handbook of Physical Properties of Rocks, I, 404 p., edited by R. S. Carmichael, CRC Press, Boca Raton, Florida, 1982

Lockhart, N. C., Electrical properties and the surface characteristics and structure of clays, I. swelling clays, J. Colloid and Interface Sci., 74, 509-519, 1980.

Lockner D. A., M. J. S. Johnston, and J. D. Byerlee, A mechanism to explain the generation of earthquake lights, Nature, 302, 28-33, 1983.

Madden, T., and R. Cantwell, Induced polarization, a review, Min. Geophys., 2, 373-400, 1967.

Madden, T., and E. Williams, Possible mechanism for stress associated with electrostatic effects, in Abnormal Animal Behavior Prior to Earthquakes, I, edited by J. Evernden, U.S. Geol. Surv., Menlo Park, Ca., 1976.

Mitzutani, H., T. Ishido, T. Yokokura, and S. Ohnishi, Electrokinetic phenomena associated with earthquakes, Geophys. Res. Lett., 3, 365-368, 1976.

Olhoeft, G. R., Electrical properties, Initial Reports on the Petrophysics Laboratory, U.S. Geol. Surv. Circ., 789, 1-25, 1979.

Shahidi M., J. B. Hasted, and A. K. Jonscher, Electrical properties of dry and humid sand, Nature, 258, 596-597, 1975.

Sumner, J. S., Principles of induced polarization for geophysical exploration, 277 pp., Elsevier Scientific Publ. Co., New York, 1976.

Wait, J. R. (Ed.), Overvoltage Research and Geophysical Applications, Pergamon Press, 1959.

Wong, J., An electrochemical model of the induced-polarization phenomenon in disseminated sulfide ores, Geophys., 44, 1245-1265, 1979.

James D. Byerlee and David A. Lockner, U.S. Geological Survey, 345 Middlefield Road, MS/977, Menlo Park, CA 94025.

(Received December 10, 1984; revised January 28, 1985; accepted February 6, 1985.)